An Analytical Approach to Evaluate the Reliability of Offshore Wind Power Plants Considering Environmental Impact

Biyang Wang, *Student Member*, *IEEE*, Xifan Wang, *Fellow, IEEE*, Xiuli Wang, *Member*, *IEEE*, Chengcheng Shao, *Student Member*, *IEEE*, Paul D. Judge, *Member, IEEE*, Tim C. Green, *Senior Member, IEEE*

***Abstract*— The accurate quantitative reliability evaluation of offshore wind power plants (OWPPs) is an important part in planning and helps to obtain economic optimization. However, loop structures in collector systems and large quantities of components with correlated failures caused by shared ambient influences are significant challenges in the reliability evaluation. This paper proposes an analytical approach to evaluate the reliability of OWPPs considering environmental impact on failures and solve the challenges by protection zone models, equivalent power unit models and common cause failure (CCF) analysis. Based on investigation of the characteristics of OWPP and related failures mechanisms, the components are divided into three CCF subsets. With the aid of the protection zone model and equivalent power unit model merged with CCF, the faulty collector system state evaluation is applied to reduce the computational burden. The case studies present the necessity and improved performance of merging CCF analysis into modeling via the comparison with other two simplified methods. A sensitivity analysis is also carried out to account for inaccuracy of failure data. The results show that the assumption of independent failures in the conventional method might lead to over-optimistic or over-pessimistic evaluation depending on the CCF style.**

***Index Terms*—offshore wind power plant; reliability evaluation; common cause failure; collector system; environmental effect**

NOMENCLATURE

A. Sets and Index

t	Index of time
q	Index of CCF order, the number of faulty components
n	Index of the total components in a system
m	Index of number of normal components
l	Index of CCF and the faulty component set
i	Index of the component
xs	Index of collector system state
pi, pj	Index of protection zone
k, h, g	Index of sum counter
$\boldsymbol{K}_q$	Event of qth-order CCF
$\boldsymbol{kc}_{q,l}$	Faulty component set corresponding to $k_{q,l}$
$Z_{q,l,i}$	Event that specified component i is fault in the lth qth-order CCF
PZ(pi)	Component set of protection zone pi
$S()$	Component set of protection zone in outage

B. Parameters, Variables and Functions

$k_{q,l}$	Element belonging to $\boldsymbol{K}_q$
$Y_{q,l,i}$	Complement of $Z_{q,l,i}$
x_i	Normal outcome of the state of component i
$Q_{n,m}$	Probability of the event that the m components work normally, $1 \le m \le n$
$P()$	Exact probability
$g_q(t)$	Probability function that qth-order CCF doesn't occur
p	Probability of component independent failure
N_q	Number of qth-order CCF occurring, q=1,2,..,n
λ_q	Failure rate of q-th order CCF
Λ	Sum of the frequency of all the CCF events
C	Total probability for the observed failure
f	Failure probability per component every time
nw	Number of power unit component
nc	Number of feeder component
nb	Number of breaker component
p_w	Probability for normal state of power unit
$Qc_{nw,c}$ $Qb_{nb,m}$ $Qw_{nw,m}$	Probability for the events that the m components operate normally in feeder, breaker and power unit component subsets respectively
nc_{pi}	Segment number of the feeders in PZ(pi)
$nc_{pi,pj}$	Number of non-breaker components in PZ(pi)∪PZ(pj)
$nb_{pi,pj}$	Number of the breakers in PZ(pi)∩PZ(pj)
$P_{PZ1}()$	Probability for first-order protection zone failure
$P_{PZ2}(,)$	Probability for second-order protection zone failure
n^*	Number of the interconnected power units in equivalent power unit model
n_1, n_2	Number of power units in equivalent model G_{E1} and G_{E2} respectively
C_w	Output capacity of each wind turbine
C_r	Capacity of path component R
C_{OWPP}	Output capacity of OWPP
$P_{OWPP}(C_{OWPP} \vert xs)$	Conditional probability for what OWPP output equals C_{OWPP} with the collector state xs given
$\lfloor\cdot\rfloor$	Floor function
m_w	Equivalent number of wind turbine connected
m_r	Equivalent number of wind turbine limited by path component
c, d, m_0, m_I	Intermediate variables

Biyang Wang, Xifan Wang, Xiuli Wang and Chengcheng Shao are with the Department of Electrical Engineering in Xi'an Jiaotong University, Xi'an, China. (email: wangbiyang1991@163.com, xfwang@ xjtu.edu.cn, xiuliw@ xjtu.edu.cn, ccshao3@ xjtu.edu.cn).

T. C. Green & Paul D. Judge are with the Department of Electrical and Electronic Engineering, Imperial College London (e-mail: t.green@imperial. ac.uk, p.judge@imperial.ac.uk).

N_q	Number of occurrences of qth-order CCF
T	Statistic period
P_q	Probability for what an qth-order CCF is observed
P_N	Probability for the occurrence of a set of N_q ($N_q = \tilde{N}_q$)
ρ	A ratio reflects the severity of multi-order CCFs and the occupation of them in all failures
$MTTR$	Mean time to repair
$N(t)$	Poisson random variable at time t
KF	The highest level of OWPP output capacity
d_{step}	Step of levels of OWPP output capacity
k_{w}	Level of OWPP output capacity in the output table
$P_{cs}(xs)$	Probability for collector system state xs
$P_{\text{OT}}()$	Exact probability or conditional probability for states in the OWPP outage table
E_{out}	Output expectation of the OWPP

C. Subscripts

w	Power unit component
c	Feeder component
b	Breaker component
$\tilde{}$	Statistic value
$\hat{}$	Estimation value

I. Introduction

Offshore wind power has developed quickly in recent years due to its high energy intensity, steady wind output and the difficulty in getting planning for onshore wind farms. The cumulative installed capacity of China reached 1.63GW in last year [1]. And the first offshore wind power plant (OWPP) in the US was installed off the Block Island in the August 2016 [2]. In Europe, 11 projects, worth €18.2bn, reached final investment decision during 2016, a 39% increase over 2015, and the total investments for the construction and refinancing hit a record level of €22.6bn [3].

Considering the high cost of investment, it is indispensable to propose a more overall reliability evaluation of OWPP. Accurate quantitative failure estimation can help obtain optimal planning, taking the tradeoff between investment and reliability into consideration. Collector systems and the Common Cause Failures (CCF) caused by severe marine environmental impact are two key points can't be neglected. However, they haven't been well considered in exiting works.

The collector system connects wind generators to the step-up substation in an OWPP. It is to some extent like a distribution system with reverse power flow, but the concerns in the reliability evaluation of it are quite different from a distribution system [4]. Its topology and breaker configuration has a significant impact on reliability [5].

Environmental conditions in OWPP are much harsher in comparison to onshore wind plants. Servicing OWPP at sea is also difficult with high maintenance expenses and limited effective construction periods [6-8]. Severe ambient influence would induce component failures, accelerate equipment aging and cause high-order correlated failure [9,10].

Works on the reliability of wind plants have usually aimed to provide estimation of output for system operator and focus on the fluctuation of wind energy [11,12]. The few works provided for planning only consider simple collector systems and are limited by topology [13]. The work in [14] adopts minimal path method to include various topologies, but the independent assumption of component failures makes it difficult to develop to consider failure relativity.

The problem widely exists in other methods to include environmental effects based on the assumption, such as multi-scenarios and failure rate modification [15-18]. The work in [15] has described the occurrence of storm carefully, and modified the independent failure rate under storm according to the wind speed. A two weather state model and a three weather state model have proposed in [16] to consider the environment impact, and an average component independent failure rate has been calculated. Similarly, the study in [17] has also modified the independent failure rate based on the hurricane forecast. Two weather states have considered in [18], and a Markov model with special failure rate of storm state has been established. All these works based on the independent assumption pay more attention to the description of multi-state weather, and the independence assumption makes the model and calculation easier and is suitable in some cases. But when it comes to OWPPs, the error introduced by the independence assumption is too significant to neglect which is alsovery hard to estimate. Thus the method proposed in this paper mainly focuses on the result caused by the environment impact, and statistical data is used, rather than weather models. It is how to consider the environmental influence that differentiate this paper from the above ones.

This paper aims to provide OWPP planning a general reliability evaluation approach which is applicable to different collector system topologies and includes the effect of harsh offshore environmental factors such as strong wind conditions, sea wave, corrosion etc.. Achieving this requires the following challenges need to be addressed: 1) closed-loop structures in collector system are hard to model by analytic methods, especially when there is non-linear calculation of series-subsystem; 2) the large number of components in OWPP makes models complicated and difficult to simplify equivalently and 3) the correlated component failures caused by the shared severe ambient impact violates the widely-used independence assumption in conventional methods. A protection zone model and an equivalent power unit model are proposed for the problem 1) and 2). In addition, a CCF analysis is adopted to account for the shared environmental effects.

CCF is the failure or abnormal state of two or more components due to a shared cause during system operation [19]. It has been used in nuclear power plants and machine industry [20,21]. Due to its complexity, the reliability model considering CCF is only used in a simple parallel- or series-system and seldom in power systems. The authors of [22] applied CCF to multi-circuit transmission configurations and developed a 2- and 3-line model by frequency and duration method. However, the number of system states becomes unwieldy when systems become larger. CCF was used in [23] to describe the earthquake effect on power system reliability via Monte Carlo simulation after the 2008 Sichuan earthquake. The simulation method makes the evaluation possible, but the computational effort was found to be extremely large. CCF has also been considered in the reliability evaluation of power sub-station [24], but more attention is paid to the concept whereas the mathematic model is not clearly presented.

This paper merges CCF analysis with an equivalent power unit model and a protection zone model via rigorous mathematical derivation and proposes a composite analytical reliability evaluation approach of OWPP. The contributions of this paper include the followings. 1) The environmental impact and the corresponding correlation among components are included. 2) The proposed approach is appropriate for different topologies of collector system. 3) The errors of the neglect of correlated component failures are discussed in details, which also verify the necessity of our work.

The rest of the paper is organized as follows. Section II discusses the characteristics of OWPP and its failures. Section III presents an overview of the theory of CCF. The protect zone model and equivalent model are proposed in Section IV, and Section V then develops the reliability model emerged with CCF analysis. The reliability calculation is presented in Section VI. And in Section VII the case studies are carried out. At last, the discussion is concluded in Section VIII.

II. Characteristics of Offshore Wind Power Plants

This section discusses the characteristics of OWPP affecting reliability, including collector system topology and failure mechanisms, with particular attentions to CCFs in OWPP.

A. Structure of OWPP and Collector System Topology

For convenience in reliability evaluation, an OWPP could be divided into three partitions: power unit, collector system and step-up substation, as shown in Fig.1(a). A power unit includes one wind turbine generator and one step up transformer. There are three types of breaker in the figure. BKR 1 represents the MV breakers connecting feeders and bus. BKR 2 is the boundary between the power unit and collector system. It could be a MV breaker, or occasionally, a fuse with LV breaker [25,26]. BKR 3 is a generator circuit breaker [27]. In collector system, only feeders and BKR 1 are discussed in this paper. The substation is installed on a platform, including bus system, step up transformers and converters with corresponding equipment if the OWPP is connected to the main grid via HVDC. Although the location of substation plays a key role in OWPP planning, its bus system topology and converter configuration do not have a strong influence on the wind turbine layout and collector system. Therefore, in order to highlight the influence of the collector system, the substation will not be discussed in this paper. A simplified example for case study is presented in Fig.1(b), in which the feeder is segmented artificially. In addition, the model in this study is not limited to AC or DC connected OWPP, and the output table of OWPP provided by this study can be applied as a multi-state component or source point in the reliability evaluation of transmission system. The reliability model of traditional transmission system has been well developed and the one of some new schemes such as multi-terminal DC system is quite complicated. Therefore this paper doesn't make further discussion and readers can refer to [28, 29] if interested.

The collector system in Fig.1 adopts the string scheme with

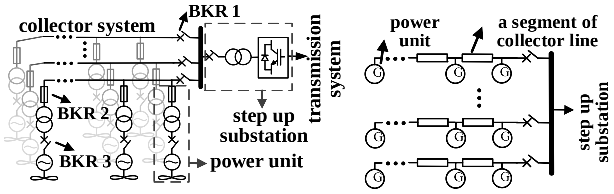

(a) a sketch of the OWPP (b) a simplified case for study

Fig.1. Sketches of the OWPP

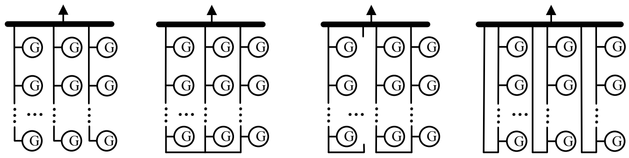
(a) string (b) general ring (c) double side ring (d) single side ring

Fig.2. Topologies of collector system (breakers omitted)

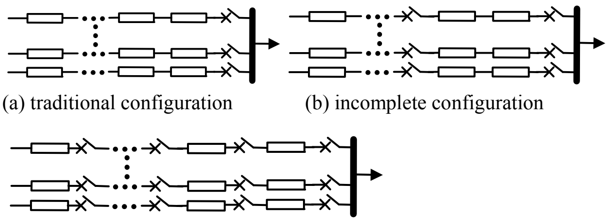
(a) traditional configuration (b) incomplete configuration

(c) complete configuration

Fig.3. Breaker configurations (Power units omitted)

traditional breaker configuration. This scheme can meet the basic functional requirements and has been widely used in many projects [30]. However, in large wind plants where the number of power units linked to one feeder can be expect to be as large as 14 or 15, this scheme may fail to satisfy the reliability targets. Thus researchers have proposed some other topologies and breaker configurations [31-33] to improve the reliability via redundancy, as shown in Fig.2 and Fig.3, in which breakers and power units are omitted separately.

Redundant topologies (e.g. general ring) could only show its superiority when combined with redundant breaker configurations: the feeder failures would be separated to avoid isolating operational power units. Although it is difficult to find detailed information about the manufacture and installation of submarine breakers, some existing works have already considered breakers in OWPP [32-34]. In order to ensure a general evaluation approach, in this paper both redundant topologies and breaker configurations are included.

B. Failures in OWPP

1) Power unit failures

Power unit failures mainly occur in the generator, gear box, bearings and power electronics. Some other common failures, caused by vibration, cooling system failure and structural damage, are introduced in the following [35].

Vibration is the large-amplitude oscillation of the tower and wind turbine engine room induced by aerodynamic braking on rotors, and yaw system over speed is the transient error due to wind gusting. These failures always last for a short period with auto reset, so is not considered in this paper.

Failures of the wind turbine cooling system would lead to wind turbine outage because of continuous heating in a long-term full-load operation with strong wind. Strong wind also raises the failure probability of some other small components (e.g. fan motor, pumps), relays and anemometers. The failures would last for a long time until they are repaired on the sea.

Structure damage mainly includes blade damage caused by flutter and tower collapse for the failures in stability, strength and the insufficiency of the pull out resistance of foundation piles. The failures are always serious and cause large loss, whose repair is costly and time-consuming.

2) Collector system failures

Failures in the collector system include the marine cable failures and breaker failures. Marine cable failures, such as core failure, major insulation damage, sheath damage etc., occur because of the imperfection in manufacture and installation, and are aggravated by the severe offshore ambient condition [36]. Most of the reported failures are caused by ship anchor dropping, pulling, seabed squeezing induced by ocean waves and localized corrosion by marine organisms [37].

Breaker failure mechanisms include false tripping and false no-tripping [38]. The breakers installed on the platform are exposed in air, and corroded by salt fog, mold and humidity.

III. Theory of Common Cause Failure

In the CCF theory, component failures are divided into *single failure* and *high-order CCF*. Because the states of components are correlated, the *system failure* is considered as an independent event in this paper rather than a collection of *component failure* in conventional method, which helps to avoid the correlation analysis and simplify the calculation.

A. Description of component and system faulty states

Two states are applied to components and systems: normal and faulty. For convenience, the single component independent failure is recorded as first-order CCF. Then let $\boldsymbol{K}_q$ denote the *event* of qth-order CCF and $k_{q,l}$ denote an element belonging to it. In a system with n components, there are n disjoint events $\boldsymbol{K}_q$, and the number of $k_{q,l}$ (q=1,2,…, l=1,2,…) is C_n^q.

Let $\boldsymbol{kc}_{q,l}$ denote the faulty *component set* corresponding to $k_{q,l}$. Then for a specified component i, the number of the $\boldsymbol{kc}_{q,l}$ including it is C_{n-1}^{q-1} ($1\le q\le n$). Let $Z_{q,l,i}$ denote the corresponding event that specified component i is fault in the lth qth-order CCF, where $1\le l\le \mathrm{C}_{n-1}^{q-1}$, and let $Y_{q,l,i}$ denote the complement of $Z_{q,l,i}$. The total number of $Y_{q,l,i}$ is $\sum_{q=1}^{n}\mathrm{C}_{n-1}^{q-1}=2^{n-1}$. Then the normal outcome of the state of component i is presented by

$$x_i=\bigcap\nolimits_{q=1}^{n}\bigcap\nolimits_{l=1}^{\mathrm{C}_{n-1}^{q-1}}Y_{q,l,i} \tag{1}$$

It is important that events $Y_{q,l,i}$ with different values of i are not mutually exclusive. With the same q, the number of events $Y_{q,l,i}$ is q times of that one of $k_{q,l}$.

B. Probability Calculation and Similar Model

If all the components in a system share the same architecture and ambient impact, then for a specified value of q, the probabilities for events $k_{q,l}$ are the same, so are the ones of all $Y_{q,l,i}$. Thus $P(Y_{q,l,i})=g_q(t)$ with all value of l.

Then according to (1), the probability for the event that the m components work normally is

$$Q_{n,1}=P(x_i)=\prod\nolimits_{q=1}^{n}\left(g_q(t)\right)^{\mathrm{C}_{n-1}^{q-1}} \tag{2}$$

$$Q_{n,m}=P(x_1)P(x_2|x_1)\cdots P(x_m|x_1x_2\cdots x_{m-1})=\prod_{k=n-m+1}^{n}Q_{k,1} \tag{3}$$

From (2) and (3), we can obtain

$$\begin{aligned}Q_{n,m}&=\prod\nolimits_{k=n-m+1}^{n}\prod\nolimits_{q=1}^{k}\left(g_q(t)\right)^{\mathrm{C}_{k-1}^{q-1}}\\&=\prod\nolimits_{q=1}^{n-m}\left(g_q(t)\right)^{\sum_{k=1}^{m}\mathrm{C}_{n-k}^{q-1}}\prod\nolimits_{q=n-m+1}^{n}\left(g_q(t)\right)^{\sum_{k=q}^{n}\mathrm{C}_{k-1}^{q-1}}\end{aligned} \tag{4}$$

If the life of components are identically exponentially distributed and share similar common cause attributes and impacts, the system can be described by Similar Model with the following properties. 1) Probabilities could be calculated by replacing p^m with $Q_{n,m}$ in the calculation based on the independent and identical distributed (i.i.d) premise. It is the called implicit method. 2) The number of qth-order CCF occurrence, N_q, is a Poisson random variable with parameter $\mathrm{C}_n^q\lambda_q$. With the aid of it, the parameter estimation and reliability evaluation become simpler. The premise is easier to satisfy than the i.i.d. one.

C. CCF Model

Several different CCF models have been developed to estimate the CCF rate, such as the multiple Greek letter model, beta factor model [39], and binomial failure rate (BFR) model, which all have different merits and shortcomings. As they don’t affect the reliability model of system, no further discussions are provided here. The BFR model is adopted here because it can estimate a lot of parameters with limited data and distinguish between partial and complete failures [19].

The sum of the frequency of all the CCF events is

$$\Lambda=\sum\nolimits_{q=1}^{n}\mathrm{C}_n^q\lambda_q \tag{5}$$

It is convenient to focus on the individual components separately. Repeat n independent experiments on every units respectively. The total probability for the observed failure is

$$C=\sum\nolimits_{q=1}^{n}\mathrm{C}_n^q f^q(1-f)^{n-q} \tag{6}$$

With the aid of conditional probability, (7) is obtained.

$$\lambda_q=\left(\Lambda\cdot f^q(1-f)^{n-q}\right)\Big/C \tag{7}$$

IV. Reliability Model of OWPP with CCF

In this section, a protection zone is proposed to open the loop structure and then an equivalent power unit model is established to simplify the calculation. The influence of environment is described by CCF merged into these two models.

According to different ambient impact conditions, the components in OWPPs are divided into three CCF component subsets: *power unit*, *feeder* and *breaker*. The CCFs between components belonging to different subsets are not considered in this paper.

A. Reliability Model for Protection Zones with CCF

The protection zone is a connecting area which is the minimum group of units that will be placed into outage in the event of a failure. Protection zones are connected to each other via one or more breakers and can be described by a component set of feeders and breakers. A typical collector system configuration is shown in Fig. 4. The breaker J belongs to both PZ(I) and PZ(II), recorded as J$\in$PZ(I)$\cap$PZ(II). In this paper, when

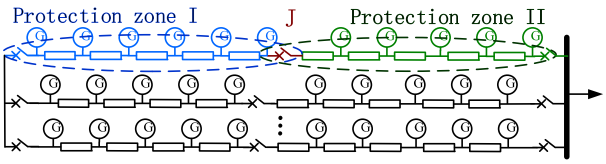

Fig. 4. Protection zone model

a false no-tripping failure occurs in breaker J, the protection zone in outage is described by S(J)=PZ(I) ∪PZ(II).

It is important to note that the protection zones do not include the power units connected to the feeder through a fuse connection. And the situation that the breakers act as a backup protection due to fuse failures is not accounted in. In essence, the state of the collector system is the combination of protection zone states.

The event that only one protection zone fails is described by first order protection zone outage. Only non-breaker component failures occur. The probability is calculated as (8).

$$P_{\mathrm{PZ1}}(pi)=\sum_{k=1}^{nci}\left(\mathrm{C}_{nci}^{k}\left(1-p_c\right)^{k}\cdot p_c{}^{nc-k}\right)\cdot p_b{}^{nb} = \sum_{k=1}^{nci}\left(\mathrm{C}_{nci}^{k}\sum_{h=0}^{k}\mathrm{C}_{k}^{h}\left(-1\right)^{h}\cdot Qc_{nc,nc-k+h}\right)\cdot Qb_{nb,nb} \tag{8}$$

Similarly, we use second-order protection zone outage to describe the event that two protection zones fail at the same time. It includes two sub-cases. 1) There is at least one faulty non-breaker component in PZ(pi) and PZ(pj) respectively while all other components operate correctly. 2) There is at least one faulty breaker in PZ(pi)∩PZ(pj) while the components out of PZ(pi)∪PZ(pj) operate correctly. Let a and b denote the probability for the two sub-cases respectively, the probability of the second-order failure is

$$P_{\mathrm{PZ2}}(pi,pj)=a+b \tag{9}$$

$$a=\sum_{k=1}^{nc_{pi}}\sum_{h=1}^{nc_{pj}}\left(\mathrm{C}_{nc_{pi}}^{k}\mathrm{C}_{nc_{pj}}^{h}\left(1-p_c\right)^{k+h}\cdot p_c{}^{nc-k-h}\right)\cdot p_b{}^{nb} = \sum_{k=1}^{nc_{pi}}\sum_{h=1}^{nc_{pj}}\left(\mathrm{C}_{nc_{pi}}^{k}\mathrm{C}_{nc_{pj}}^{h}\sum_{g=0}^{k+h}\mathrm{C}_{k+h}^{g}\left(-1\right)^{g}Qc_{nc,nc-k-h+g}\right)\cdot Qb_{nb,nb} \tag{10}$$

$$b=\sum_{k=1}^{nb_{pi,pj}}\left(\mathrm{C}_{nb_{pi,pj}}^{k}\left(1-p_b\right)^{k}\cdot p_b{}^{nb-k}\right)\cdot p_c{}^{nc-nc_{pi,pj}} = \sum_{k=1}^{nb_{pi,pj}}\left(\mathrm{C}_{nb_{pi,pj}}^{k}\sum_{h=0}^{k}\mathrm{C}_{k}^{h}\left(-1\right)^{h}Qb_{nb,nb-k+h}\right)\cdot Qc_{nc,nc-nc_{pi,pj}} \tag{11}$$

B. Reliability Model for Equivalent Power Unit with CCF

The term Wind Turbine String is applied to describe a feeder and the power units connected to it here. In the collector system including closed-loop structure, the feeder not only provides transmission capacity for wind generators in its own string, but also for the ones belonging to others as backup.

The series and parallel analysis can properly describe the reliability relationship of components in a system and is convenient for further study, which is extensively adopted. However, the following difficulties arise when the method is applied directly. 1) It would fail in closed-loop topology; 2) It is hard to simplify the series and parallel crossed calculation. Therefore, in a given collector system state, an equivalent power unit model is proposed. The procedure is illustrated in Fig.5 to derive the equivalent power unit model .

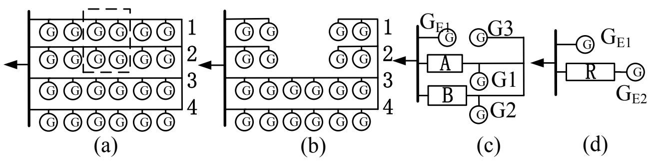

Fig. 5. Process of equivalent power unit modeling

1) Remove the protection zones in outage and the power units connected to them (shown in the dash line box in Fig.5(a)) and obtain the reduced one as shown in Fig.5(b).

2) Divide the power units in Fig.5(b) into three categories. Type I, delivering power via their own feeders which don't provide transmission capacity for power units connected to other feeders, such as the most left two power units connected Feeder 1 and 2. They are modeled by $\mathrm{G_{E1}}$ equivalently in Fig.5(c). Type II, which includes unit incapable of delivering power via their own feeders, such as the most right two power units connected to Feeder 1 and 2. They are modeled by G3 equivalently. Type III, whose own feeders work well and share transmission capacity with type II power units, such as the power units connected to Feeder 3-6. They are modeled by to G1-G3 equivalently.

3) Use *path components,* such as A and B in Fig.5(c), to describe the transmission capacity of feeders. The path component is an abstract lumped model of feeders. It is series connected between the bus and Type III equivalent power unit. Thus its capacity limits the transmission capacity of the feeder.

4) An equivalent power unit $\mathrm{G_{E2}}$ and path component R can be obtained via twice parallel calculations of the interconnected Type II, Type III equivalent power units and the path components A, B respectively, as shown in Fig.5(d). $\mathrm{G_{E1}}$ and $\mathrm{G_{E2}}$ are two types of equivalent power unit model.

The reliability model of collector system can then be described by one $\mathrm{G_{E1}}$, several $\mathrm{G_{E2}}$ and path components with the equivalent power unit model applied. The loop structure is opened equivalently at the same time.

The reliability of power unit could be represented by a two state output table. The linear model is applied to describe the output of wind generator, and the approach in [40] is applied to calculate the weak effect. Thus the output outage table of equivalent power unit model can be obtained by parallel calculation of all power units belonging to it, and the conditional probability of output can be calculated as follows.

$$P_{\mathrm{OWPP}}(C_{\mathrm{OWPP}}|xs)=\begin{cases} c & m_{\mathrm{w}}<m_r \\ c+d & m_{\mathrm{w}}\ge m_r \end{cases},\quad \begin{matrix} m_{\mathrm{w}}=\lfloor C_{\mathrm{OWPP}}/C_{\mathrm{w}}\rfloor \\ m_{\mathrm{r}}=\lfloor C_{\mathrm{r}}/C_{\mathrm{w}}\rfloor \end{matrix} \tag{12}$$

$$\begin{cases} c=\sum_{k=0}^{m_0}\mathrm{C}_{n_2}^{k}\mathrm{C}_{n_1}^{m_{\mathrm{w}}-k}p_{\mathrm{w}}{}^{m_{\mathrm{w}}}\left(1-p_{\mathrm{w}}\right)^{n^*-m_{\mathrm{w}}} \\ d=\sum_{k=m_{\mathrm{r}}}^{n_2}\mathrm{C}_{n_2}^{k}\mathrm{C}_{n_1}^{m_1}p_{\mathrm{w}}{}^{m_1+k}\left(1-p_{\mathrm{w}}\right)^{n^*-(m_1+k)} \end{cases} \tag{13}$$

$$m_0=\min\{m_{\mathrm{w}},m_{\mathrm{r}}-1\},\qquad m_1=m_{\mathrm{w}}-m_{\mathrm{r}}$$

Note that the unconnected power units can also be in outage due to CCFs. The total number of turbines is still nw rather than n^* in the CCF analysis. Thus (13) can be rewritten as (14) with the aid of implicit method of similar model.

$$\begin{cases} c=\sum_{k=0}^{m_0}\mathrm{C}_{n_2}^{k}\mathrm{C}_{n_1}^{m_i-k}\sum_{h=0}^{n^*-m_i}\mathrm{C}_{n^*-m_i}^{h}\left(-1\right)^{h}Qw_{nw,h+m_i} \\ d=\sum_{k=m_r}^{n_2}\mathrm{C}_{n_2}^{k}\mathrm{C}_{n_1}^{m_1}\sum_{h=0}^{n^*-(m_1+k)}\mathrm{C}_{n^*-(m_1+k)}^{h}\left(-1\right)^{h}Qw_{nw,h+m_1+k} \end{cases} \tag{14}$$

V. Reliability Calculation

This section firstly discusses the parameter estimation of CCF and then presents a method of reliability index calculation. The whole reliability evaluation approach proposed in this paper is illustrated by a flow chart in Part C.

A. Estimation of CCF Parameters

In the reliability evaluation of OWPP, the available statistical data includes: the number of occurrences of qth-order CCF denoted by $\tilde{N}_q$ and the statistic period denoted by T. Then the unbiased estimation of the Λ in (7) can be obtained by

$$\hat{\Lambda} = \left(\sum_{q=1}^{n} \tilde{N}_q\right) \Big/ T \tag{15}$$

In the BFR model, the probability corresponding to what an qth-order CCF is observed can be calculated as

$$P_q = \left(\mathrm{C}_n^q f^q (1-f)^{n-q}\right) \Big/ C \tag{16}$$

Thus the probability corresponding to what a set of N_q ($N_q = \tilde{N}_q$) occur is

$$P_N = P\left(N_q = \tilde{N}_q, q = 1, \cdots, n\right) = \tilde{N}_q ! \prod_{q=1}^{n}\left(P_q^{\tilde{N}_q} \Big/ \tilde{N}_q !\right) \tag{17}$$

The Maximum Likelihood solution of parameter f is

$$\ln P_N = \ln \tilde{N}_q ! + \sum_{q=1}^{n}\left(\tilde{N}_q \ln P_q - \ln \tilde{N}_q !\right) \tag{18}$$

Then the Maximum Likelihood estimation of f is

$$\hat{f} = \left(\sum_{q=1}^{n} q \cdot \tilde{N}_q\right) \Big/ \left(n \cdot \sum_{q=1}^{n} \tilde{N}_q\right) \tag{19}$$

where $\sum_{q=1}^{n}(q \cdot \tilde{N}_q)$ and $\sum_{q=1}^{n}\tilde{N}_q$ are the sum of faulty items of all failures and the sum of failures respectively. Let ρ denote the ratio of these two,

$$\rho = \left(\sum_{q=1}^{n} q \cdot \tilde{N}_q\right) \Big/ \left(\sum_{q=1}^{n} \tilde{N}_q\right) \tag{20}$$

then ρ could reflect the severity of multi-order CCFs and the occupation of them in all failures. It is applied in case study to consider data error.

With the unbiased estimation of C obtained by (6), the CCF rate λ_q can be calculated by (7). However, it is interesting that $\mathrm{C}_n^q \lambda_q$ is much more valuable than λ_q in the analysis since the former can reflect the frequency of all qth-order CCF more directly. The $g_q(t)$ is calculated by

$$g_q(t) = 1 - \left(\lambda_q \times MTTR\right) \Big/ 8760 \tag{21}$$

where $MTTR$ denotes the mean time to repair.

In order to analyze the influence of ρ on λ_q, keep the $\sum_{q=1}^{n}(q \cdot \tilde{N}_q)$ being fixed and calculate the partial derivative of $\ln(\lambda_q)$ with respect to $\hat{f}$ (because $\rho = \hat{f} \times n$),

$$\frac{\partial \ln \lambda_q}{\partial \hat{f}} = \frac{q - n \cdot \hat{f} - q \cdot \left(1-\hat{f}\right)^n}{\hat{f} \cdot \left(1-\hat{f}\right) \cdot \left(1-\left(1-\hat{f}\right)\right)^n} \tag{22}$$

According to (22), when $\hat{f}(\rho)$ rises, the change of λ_q is dependent on the value of q. It will decrease with a low m and increase if the value of q is large. In addition, the exponents of the $g_q(t)$ in (4), $\sum_{k=1}^{q}\mathrm{C}_{n-k}^{q-1}$ and $\sum_{k=q}^{n}\mathrm{C}_{k-1}^{q-1}$, increase at first and then falls with the rise of q. Thus when the $\sum_{q=1}^{n}(q \cdot \tilde{N}_q)$ is fixed, the increase of ρ will not always lead to the drop of reliability. This will be further discussed in Section VI.

If all the failures are considered to be independent, then the component failure occurrence can be modelled as a Poisson Process. Neglecting the maintenance period and setting the Poisson random variable at initial time $N(0)=0$ results in the following expression for

$$P\left(N(T)\right) = \left((\lambda T)^{\sum_{q=1}^{n} q \cdot \tilde{N}_q}\right) \Big/ \left(\left(\sum_{q=1}^{n} q \cdot \tilde{N}_q\right)! \cdot e^{-\lambda T}\right) \tag{23}$$

With the aid of Maximum likelihood estimation, the independent failure rate λ can then be estimated by

$$\hat{\lambda} = \left(\sum_{q=1}^{n} q \cdot \tilde{N}_q\right) \Big/ T \tag{24}$$

Compared with the reliability calculation considering CCF, the high-order component failures are underestimated when all the failures are assumed to be independent, which could be proved via the implicit method and (4), (15)-(20) and (23). It will be discussed in Section VI by case study but the corresponding mathematical derivation is not presented.

B. Calculation of System Reliability

Here the faulty state evaluation of the collector system is adopted thanks to the proposed protection model and equivalent power unit model. The total number of states is an exponential function and the number of components in system is the exponent, and power units account for 30%-50% of all the components in OWPPs in reliability study (as shown in Fig.4). Therefore, the amount of the collector system states (not including power units) is a lot fewer than that of components in the whole system, which is usually used in the conventional faulty state evaluation. For example, in an OWPP with 134 wind turbines and 12 feeders in string topology and traditional breaker configuration, the number of states to evaluate is reduced from 3244409 to 91. Thus the models proposed in section IV help to reduce the computational burden.

The output capacity of OWPP can be divided into several levels from 0 to KF with a step d_{step}. The corresponding output level denoted by k_{w} can be calculated by (25).

$$\begin{aligned} &P_{\mathrm{OT}}\left(k_{\mathrm{w}} \mid xs\right) = \sum P_{\mathrm{OWPP}}\left(C_{\mathrm{OWPP}} \mid xs\right), \\ &\text{where } \left(k_{\mathrm{w}} - 0.5\right) \cdot d_{\mathrm{step}} \le C_{\mathrm{OWPP}} < \left(k_{\mathrm{w}} + 0.5\right) \cdot d_{\mathrm{step}} \end{aligned} \tag{25}$$

Based on the *outage table* obtained for each faulty collector system state, the total outage table and the reliability indexes can be obtained according to the formula of total probability. The probability corresponding to the collector system state xs, $P_{\mathrm{cs}}(xs)$, equals to $P_{\mathrm{PZ1}}(i)$ or $P_{\mathrm{PZ2}}(i,j)$ according to (8)-(11) in Section IV. Then the exact probability for the output being k_{w} in the system outage table can be calculated by

$$P_{\mathrm{OT}}\left(k_{\mathrm{w}}\right) = \sum_{xs=1}^{ns} P_{\mathrm{OT}}\left(k_{\mathrm{w}} \mid xs\right) P_{\mathrm{cs}}\left(xs\right) \tag{26}$$

In this way, the complete system outage table can be obtained as well as the output expectation of the OWPP E_{out}.

$$E_{\mathrm{out}} = \sum_{k_{\mathrm{w}}=1}^{KF}\left(k_{\mathrm{w}} \cdot d_{\mathrm{step}} \cdot P_{\mathrm{OT}}\left(k_{\mathrm{w}}\right)\right) \tag{27}$$

In practice, since the probability of third- or higher-order protection zone outages are extremely small (always $<10^{-4}$ in our study), the corresponding cases are not included.

E_{out} is the main reliability metric in this paper. Different from a device or component, OWPP is a system with multiple output states. Thus the probability index E_{out} can present the reliability of OWPP more obviously. However, the probability of some special states, $P_{\mathrm{OWPP}}(k_{\mathrm{w}})$, are also important in further

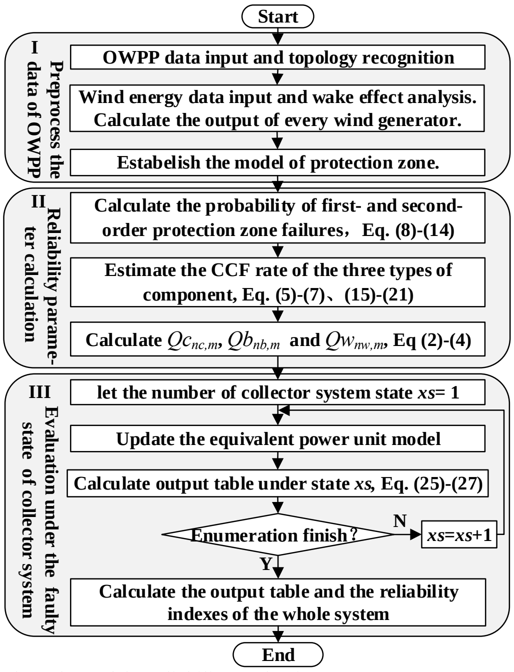

Fig. 6. Flow chart of the reliability evaluation

analysis. $P_{\mathrm{OWPP}}(k_{\mathrm{w}})$ is a kind of availability metric of state k_{w}.

C. Flow chart of the reliability evaluation

The flow chart of the proposed reliability evaluation is shown in Fig. 6. The process consists of three main parts, OWPP data pre-processing, reliability parameter calculation and the evaluation under faulty state of collector system. The modeling of protection zones in part I and part II is used to open the loop structures and help in analytical method application. The dynamic modeling of equivalent power unit in part III is used to simplify the calculation. And environmental impact is considered via CCF analysis during modeling.

VI. Case Study

A. Sample System and Reliability Data

An OWPP based on a project in China is used as a case study. The string scheme collector system and traditional breaker configuration are applied. The project contains 40 wind turbines connected to 6 feeders, each with a capacity of 5 MW. Each feeder capacity is 70MW and the number of wind turbines connected to each feeder is 7, 7, 6, 7, 6 and 7 respectively. The distance between the adjacent turbines on the same feeder is 800m and the distance between the feeders is 800m. The overall layout of the OWPP is shown in Fig. 7.

For the wind turbine, the cut-in, rated and cut-off speed is 3m/s, 12m/s and 25m/s respectively. Here in order to highlight the effect of the collector system and CCF, only the case that the wind blows from east at a speed of 25m/s is considered.

The reliability parameters of components and the failure statistics are shown in Table I and Table II respectively. The data in Table I are those one of independent faults, referred to [41-43]. The failure rate data of generators in OWPPs was discussed carefully in [41] according to reference and reports from OWPP in UK, Denmark and China. Although the data varied with different cases, it was concluded that "the availability of generator is over 90% in total, and about 93.5%-95.9% in China". In contrast to the data in [43], it was indicated in [41] that most generator failures didn't last for a long time and could be reset automatically. It is in correspondence with what has been discussed in Section III in this paper, and the failure rates is quite higher than that of the onshore wind power plants referred to [44]. The failure rate of the breaker and bus is referred to [42], but considering the difficulties of repair in OWPP, the MTTR is referred to [43]. The reliability parameter of feeders is also referred to [43] but the failure rate is modified because of length. Part of the data in Table II is obtained from [45]. The data in [45] was obtained under typhoon conditions, which is not strictly suitable in this case, because the long term performance is emphasized in this paper. But there are few reference on CCF statistics, so we complete and slightly modify the data in corresponding with the failure rates in Table I according to the calculation and research experience of CCF applied in machinery and nuclear power plant field, referred to [46]. Furthermore, in order to assess the inaccuracy carried by the data process method, a *sensitivity analysis* is carried out to discuss the influence of data error in Table II on results. With the same failure rate value, the characteristics of data in Table II can be presented by ρ obtained by (20).

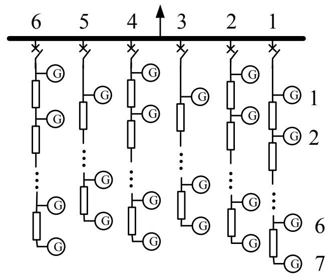

Fig. 7 An offshore wind power plant with string topology for case study

TABLE I
Reliability Parameters of Components

Component	Failure rate/int·y^{-1}	Availability/%	MTTR/h
Power Unit	50.225	93.120	12
Breaker	0.032	99.912	240
Feeder	0.0025	99.959	1440
Bus	0.598	98.362	240

TABLE II
Common cause failure statistics

Component	q	$\tilde{N}_q$	q	$\tilde{N}_q$	q	$\tilde{N}_q$
	1	1880	5	4	6	4
Power Unit	7	4	18	1	19	1
	20	1				
Breaker	1	0.12	3	0.01	6	0.007
	1	0.06	5	0.001	6	0.001
Feeder	7	0.001	11	0.0001	12	0.0001
	13	0.0001	16	0.0001	17	0.0001

B. Basic analysis of sample system

The OWPP in Fig.7 has 7 protection zones, as shown in Fig.8 (a). There are only Type I equivalent power unit in the sample system, as G_{E1} shown in Fig.8 (b). According to the number of generator included in equivalent power unit, the corresponding collector system state could be divided into 6 groups, which is presented in Table III. As shown, the failures of bus and breakers which are belong to PZ(VII) will lead to a sever outage, whole system down.

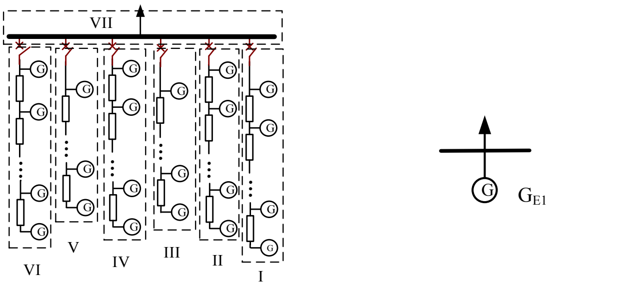

(a) protection zone model (b) equivalent power unit model

Fig. 8 Protection zone and equivalent power unit model of sample system

TABLE III
COLLECTOR SYETM STATE AND CORRESPONDING EQUIVALENT POWER UNIT

No.	Collector System State	Number of generators in G_{E1}
1	First-order outage of Protection zone I, II, IV or VI	33
2	First-order outage of Protection zone III or V	34
3	Second-order outage of 2 protection zones selected from I, II, IV, VI	26
4	Second-order outage of 2 protection zones, one selected from I, II, IV, VI and one from III or V	27
5	Second-order outage of protection zones III and V	28
6	All states with outage of protection zone VII	0

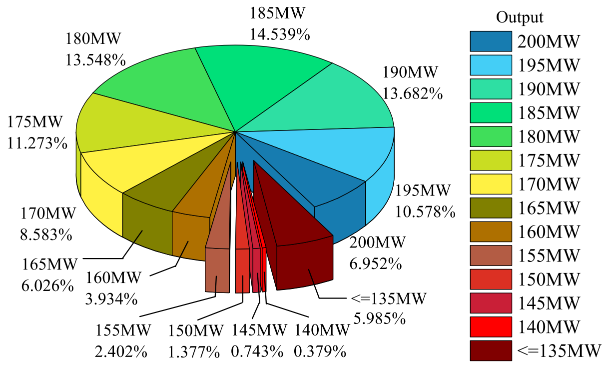

Fig. 9. Pie chart of outage table

The results of CCF rate estimation is presented in the Appendix, in which the $C_n^q \lambda_q$ lower than 10^{-8} are not listed. As shown, power units are the component which are most likely to suffer from CCFs, although most of them are lower-order ones. But when it comes to the feeder, third-order and forth-order CCF have higher occurrence frequencies.

The outage table is listed in Table A-II in Appendix and described in Fig.9 via a pie chart. The blue and green sectors present the cases with high output and corresponding high availability, higher than 180MW. The cases only take about half of the whole. The yellow parts are the cases whose availability is only 160MW-180MW (80%-90% of the rated capacity). Collector system failures always lead to severe outage in this OWPP, corresponding to the wine red sector (≤135MW) in the figure, account for 5.98%.

C. Comparison of three methods

The three methods listed in Table IV are compared here.

Firstly, the reliability evaluation results are presented via E_{out}, outage table in Table V and Table A-II in the Appendix respectively. The E_{out} of method 2 is the highest, 4% higher than that of method 3 and 7% higher than that of method 1. It means that the neglect of correlated failures will lead to over

TABLE IV
THREE METHODS IN COMPARISON

Name	Description
Method 1	CCF considered, the method proposed in this paper
Method 2	Only the independent failures considered (λ_q=0, q>1)
Method 3	All failures assumed to be independent (conventional method)

TABLE V
THREE METHODS IN COMPARISON

Index	Method 1	Method 2	Method 3
E_{out}	170.1886MW	182.6393MW	175.6613MW

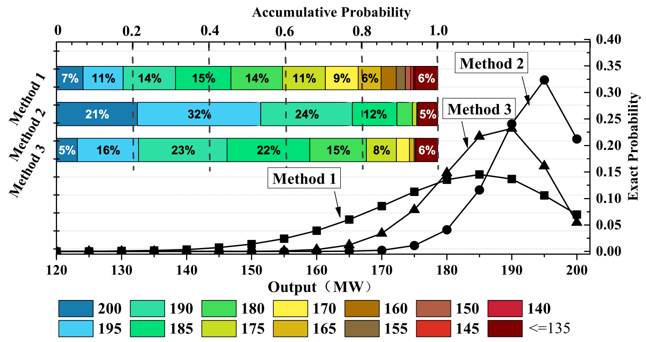

Fig. 10. Output probability distributions by different methods

estimation of reliability. Comparing exact probability of method 1 and method 3 in the outage table, we can find that most probable output of method 3 is centralized in 180MW-195MW, but the one of Method 1 is in a wider interval. This is obviously presented by bars and lines in Fig. 10.

In Fig. 10, the bars present the accumulative probability of output and the lines describe the exact probability. As shown, the distribution of exact probability obtained by Method 1 (CCF considered) appears to be very gentle and smooth and the size of different color blocks in accumulative probability bar are similar. It implies that the rates of different order failures are similar and higher-order power unit failures are easier to occur with CCF considered. For Method 2 (only the independent failures considered), the probability increases sharply at the tail of the distribution curve and the blue blocks take a big occupation in the colorful bar. It means that with only independent failures considered there are only first- and second-order power unit failures in most situations. The shape of the distribution obtained by Method 3 (all failures assumed to be independent) is similar to that by Method 1, but with a sharper rise at higher power levels, and the size of green blocks (representing the probability of cases when output is between 180-190MW) increases significantly. Thus neglecting the relativity of failures can put more probability onto the cases with only 1-4 faulty power units. The yellow and red blocks (representing the serious outage that the output tis lower than 135MW) become much smaller, that is to say the probability for severe failures with more power units breaking down is under estimated. Therefore, it is important and necessary to include CCF especially for the extreme condition analysis.

Secondly, here we make a simple discussion about the calculation time. The most important premise is that all the methods discussed in the case study are analytical methods. The most time-consuming part in analytical methods is usually the state enumeration, which is one of their main limits of application. However, in our work, the number of states is effectively

TABLE VI
VALUE OF ρ OF SEVEN DATASETS

Dataset	1	2	3	4	5	6	7
ρ	1.06105	1.29446	1.60592	1.82803	2.24219	2.83750	3.11473

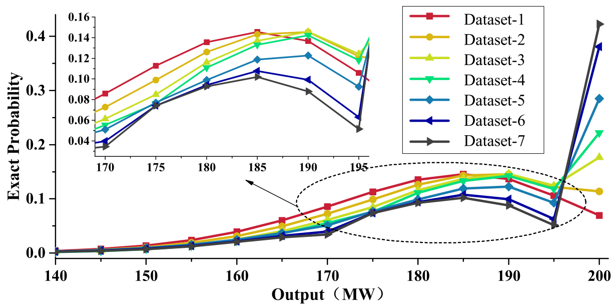

Fig. 11. Output probability curves with varying ρ

TABLE VII
OUTPUT EXPECT OF SEVEN CASES

Dataset	1	2	3	4	5	6	7
E_{out}/MW	170.189	172.280	174.253	175.366	175.670	177.254	177.973

decreased by the protection zone model and equivalent power unit model (from 3321 to 29 in the sample system). In the comparison of the three methods, method 1 is the most algorithmically complex in the calculation of reliability parameter, part II in Fig.6. In spite of this, the calculation only takes several seconds (using Intel Visual Fortran 2011), and the time is mostly spent on the estimation of CCF rate.

D. Sensitivity analysis

In order to account for the inaccuracy of failure data and reliability parameter, the sensitivity of the system reliability is analyzed. The analysis will show the variation of reliability evaluation results when failure data change. The change is presented by the varying ρ ($\sum_{q=1}^{n}(q\cdot\tilde{N}_q)$ is fixed in this study). Besides, it also presents the trend that reliability change with the environmental impact.

There are 7 datasets considered here, the value of ρ is shown in Table VI. However, because $\sum_{q=1}^{n}(q\cdot\tilde{N}_q)$ is fixed, the increasing of ρ doesn't mean that the higher-order CCFs occur more frequently. On the contrary, the total number of failures ($\sum_{q=1}^{n}\tilde{N}_{q}$) decreases with the change. Thus it is necessary to notice that, the value of ρ just describe the type of CCF that is faced rather than the severity of the CCF.

The output distributions are shown in Fig. 1. The shape of curves are similar as ρ increases, but the tail of dark curves in full-output case rise due to the decreasing of $\sum_{q=1}^{n}\tilde{N}_q$.

The output expect E_{out} of the seven cases are presented in Table VII. Comparing with the one of method 3 (conventional method, E_{out}=175.6613MW), we can find that when the ρ is low and higher-order CCFs take up a small percentage, the E_{out} is lower than that obtained by method 3. In that case the reliability will be over-estimated if the independent assumption is applied. On the contrast, if the higher-order CCFs occur frequently compared with lower-order CCFs, then the results will be under-estimated.

VII. CONCLUSION

This paper has proposed an analytical approach to evaluate the reliability of offshore wind power plants (OWPPs). The method is applicable to different collector system topologies and breaker configurations thanks to the proposed protection zone model and equivalent power unit model. Environmental impact is also included via the Common Cause Failure (CCF) analysis. The reliability model combined with faulty state evaluation of collector system can reduce the computational burden efficiently, and obtain reliability indexes and outage table. The method of CCF parameters estimation is presented as well as the discussion on the error and sensitivity analysis. The reliability evaluation method is compared with other two simplified methods in a case study. The results show the necessity to include environmental impact and the relativity of failures. The assumption independent failures might lead to over-optimistic or over-pessimistic evaluation depending on the CCF style. The proposed approach can also throw some light on the reliability evaluation of bus stations and some transmission systems.

APPENDIX

TABLE A-I
RESULT OF CCF PARAMETER ESTIMATION

Component	q	λ_q/ int·y^{-1}	$C_n^q\lambda_q$/ int·y^{-1}	q	λ_q / int·y^{-1}	$C_n^q\lambda_q$ / int·y^{-1}
Power Unit	1	2.675e+01	1.070e+03	2	7.283e-1	5.681e+02
	3	1.982e-02	1.959e+02	4	5.397e-04	4.932e+01
	5	1.469e-05	9.666e+00	6	3.999e-07	1.535e+00
	7	1.089e-08	2.029e-01	8	2.963e-10	2.279e-02
	9	8.066e-12	2.206e-3	10	2.196e-13	1.8615e-3
	11	5.977e-15	1.382e-5	12	1.627e-16	9.090e-7
	13	4.429e-18	5.330e-8			
Breaker	1	6.528e-6	5.875e-5	2	1.194e-6	4.297e-5
	3	2.183e-7	1.834e-5	4	3.991e-8	5.029e-6
	5	7.298e-9	9.196e-7	6	1.335e-9	1.121e-7
Feeder	1	2.591e-7	9.588e-7	2	3.288e-8	2.190e-5
	3	4.173e-9	3.242e-5	4	5.295e-10	3.497e-5
	5	6.720e-11	2.929e-5	6	8.528e-12	1.982e-5
	7	1.082e-12	1.114e-5	8	1.373e-13	5.302e-6
	9	1.743e-14	2.168e-6	10	2.211e-15	7.703e-7
	11	2.806e-16	2.399e-7	12	3.561e-16	6.597e-8
	13	4.520e-18	1.610e-8			

TABLE A-II
OUTAGE TABLE

Output	Exact Probability			Accumulative Probability		
/MW	Method 1	Method 2	Method 3	Method 1	Method 2	Method 3
200	0.0695	0.2123	0.0545	1.0000	1.0000	1.0000
195	0.1058	0.3237	0.1610	0.9305	0.7877	0.9455
190	0.1368	0.2406	0.2320	0.8247	0.4639	0.7845
185	0.1454	0.1161	0.2171	0.6879	0.2234	0.5525
180	0.1355	0.0409	0.1484	0.5425	0.1072	0.3353
175	0.1127	0.0112	0.0789	0.4070	0.0663	0.1870
170	0.0858	0.0025	0.0340	0.2943	0.0550	0.1080
165	0.0603	0.0005	0.0122	0.2084	0.0525	0.0740
160	0.0393	0.0001	0.0037	0.1482	0.0521	0.0618
155	0.0240	0.0000	0.0010	0.1089	0.0520	0.0581
150	0.0138	0.0000	0.0002	0.0848	0.0520	0.0571
145	0.0074	0.0000	0.0000	0.0711	0.0520	0.0569
140	0.0038	0.0000	0.0000	0.0636	0.0520	0.0568
≤135*	0.0598	0.0520	0.0568			

*The exact probability of the items lower than 135MW are presented together, but the accumulative probability of item "≤135MW" makes no sense.

ACKNOWLEDGMENT

This work is supported by the National Natural Science Foundation of China (NSFC) (51307136) and State Grid Corporation in China under Grant (52094016000C).

Paul D. Judge (e-mail: p.judge@ic.ac.uk) would like to acknowledge financial support of the Engineering & Physical Science Research Council UK through the RESTORES project (grant number: EP/L014351/1).

REFERENCES

[1] GWEC, "Global offshore wind capacity reaches 14.4GW in 2016", 2017. [Online]. http://www.gwec.net/global-offshore-wind-capacity-reaches-14-4gw-in-2016/

[2] F. Katie, "The first U.S. offshore wind turbines were just in-stalled", 2016. [Online]. http://fortune.com/2016/08/08/first-us-offshore-wind/

[3] Wind Europe, "The European offshore wind industry. Key trends and statistics 2016", 2017. [Online]. https://windeurope.org/wp-content/uploads/files/about-wind/statistics/WindEurope-Annual-Offshore-Statistics-2016.pdf

[4] K. G. Boroojeni, et al, *Reliability in Smart Grids, Smart Grids: Security and Privacy Issues*. Springer International Publishing, 2017, pp. 19-29.

[5] E, H Camm, M, R Behnke, O, Bolado, M. Bollen, et al, "Wind power plant substation and collector system redundancy, reliability, and economics", *2009 IEEE Power & Energy Society General Meeting*, 2009.

[6] Besnard F, Fischer K, Tjernberg L B, "A model for the optimization of the maintenance support organization for offshore wind farms". *IEEE Trans. Sustainable Energy,* vol.4, no.2, pp.443-450, 2013.

[7] Tavner P. *Offshore Wind Turbines: Reliability, availability and maintenance*, The Institution of Engineering and Technology, London, 2012.

[8] Maurer R. "Power under the sea". 2014. [Online]. http://www.agcs.allianz.com/assets/PDFs/GRD/GRD%20individual%20articles/022014/SpecialTopicWater_power-under-the-sea.pdf

[9] X. Liu, T. Zhang, R. Zhang, et al. "The effect of the marine environment on the stator insulation system of an offshore wind turbine generator", *IEEE Electrical Insulation Magazine*, vol.31, no.3, pp.10-17, 2015.

[10] X. Liu, T. Zhang, R. Zhang, et al. "Experimental research on stator insulation system of 5 MW offshore wind turbine generator under simulated marine environments", *2013 Annual Report Conference on Electrical Insulation and Dielectric Phenomena*, 2013.

[11] H. Yang, K. Xie, H. M Tai, et al. "Wind Farm Layout Optimization and Its Application to Power System Reliability Analysis". *IEEE Trans. Power Systems*, vol.31, no.3, pp.2135-2143, 2016,.

[12] H. Kim, C. Singh, A. Sprintson. "Simulation and Estimation of Reliability in a Wind Farm Considering the Wake Effect". *IEEE Trans. Sustainable Energy*, vol.3, no.2, pp.274-282, 2012.

[13] L. He, M. Zhou, F. Guo, et al. "Comparative study on reliability of wind farm collector systems", *International Conference on Renewable Power Generation (RPG 2015)*, 2015.

[14] O. Dahmani, S. Bourguet, M. Machmoum, et al. "Optimization and reliability evaluation of an offshore wind farm architecture". *IEEE Trans. Sustainable Energy*, 2016, early access.

[15] G. Li, P. Zhang, P. B Luh, et al. "Risk Analysis for Distribution Systems in the Northeast U.S. Under Wind Storms". *IEEE Trans. Power Syst.*, vol.29, no.2, pp.889-898, 2014.

[16] R. Billinton. J. Acharya, "Consideration of multi-state weather models in reliability evaluation of transmission and distribution systems", *Canadian Conference on Electrical and Computer Engineering*, 2005.

[17] Y. L, C. S. A, "Methodology for evaluation of hurricane impact on composite power system reliability," *IEEE Trans. Power Syst.*, vol.26, no.1, pp.145-152, 2011.

[18] Sarwat, Arif I., et al. "Smart Grid reliability assessment utilizing Boolean Driven Markov Process and variable weather conditions." *North American Power Symposium (NAPS)*, IEEE, 2015.

[19] C. N. Guey, *A method for estimating common cause failure probability and model parameters*, MIT Energy Laboratory Report, 1984.

[20] P. Kvam, "A parametric mixture-model for common-cause failure data of nuclear power plants". *IEEE Trans. Reliability*, vol.47, no.1, pp.30-34,1998.

[21] *IEC/IEEE Standard for Nuclear facilities Electrical equipment important to safety Qualification*, IEC/IEEE Standard, 20161-70.

[22] Billinton R, Medicherla T K P, Sachdev M S., "Common-cause outages in multiple circuit transmission lines," *IEEE Trans. Reliability*, vol.27, no.2, pp.128-131, 1978.

[23] H He, J Guo. "Seismic disaster risk evaluation for power systems considering common cause failure," *Proceedings of the CSEE*, vol.32, no.28, pp.44-54, 2012. (in Chinese)

[24] Yoong-Tae B, Kiryang K, Jin-O K, "Reliability analysis of power substation with common cause failure," *2009 International Conference on Power Engineering, Energy and Electrical Drives*, pp.467-472, 2009.

[25] Dough Jones and Kyle Bennett, "Wind Farm Collector Protection using Directional Overcurrent Elements", *2012 IEEE Power & Energy Society General Meeting*, 2012.

[26] D. Smugala, W. Piasecki, M. Ostrogorska, et al. "Wind Turbine Transformers Protection Method Against High-Frequency Transients". *IEEE Trans. Power Delivery.*, vol.30, no.2, pp.853-860, 2015.

[27] Malati Chaudhary, Sukumar M. Braham and Satish J. Ranade, "Circuit Breaker Selection in a Wind Farm with Type-2 Wind Turbine Generators", *2013 IEEE Power & Energy Society General Meeting*, 2013.

[28] B Wang, X Wang, X Wang, et al. "Reliability Evaluation of VSC-MTDC Integrated Offshore Wind Plants", *IET Renewable Power Generation*, vol.10, no.6, pp.761-766, 2016.

[29] J Guo, X Wang, Z Bie, "Reliability modeling and evaluation of VSC-HVDC transmission systems", *2015 IEEE Power & Energy Society General Meeting*, 2015.

[30] Y Wu, C Lee, G Shu, "Taiwan's first large-scale offshore wind farm connection, A real project case study with a comparison of wind turbine", *IEEE Trans. Ind. Appl.*, vol.47, no.3, pp.1461-1469, 2011.

[31] Oriol G., Jun L., Janaka E., "Topologies of multiterminal HVDC-VSC transmission for large offshore wind farms", *Electric Power Systems Research*, vol.81, no.2, pp.271-281, 2011.

[32] Shadi C, Ahmadreza T., Zahra M., et al., "Topology design for collector systems of offshore wind farms with pure DC power system", *IEEE Trans. Industrial Electronics*, vol.61, no.1, pp.320-328, 2014.

[33] Francesco C., Camillo G., Paolo M., et al., "Reliability of collection grids for large offshore wind parks", *2011 8th International Conference on the European Energy Market (EEM)*, Zagreb, pp.281-287, 2011.

[34] R. S, Vinatha U., "Electrical collector topologies for offshore wind power plants: A survey," *2015 IEEE 10th International Conference on Industrial and Information Systems (ICIIS)*, pp.338-343, 2015.

[35] Bill C P L, Eden W M M, M. P. "Review of offshore wind turbine failures and fault prognostic methods", *Proceedings of the IEEE 2012 Prognostics and System Health Management Conference*, Beijing, 2012.

[36] Worzyk T. *Submarine power cables: design, installation, repair, environmental aspects*. Springer Dordrecht Heidelberg, London, 2009.

[37] EMEC. "PFOW enabling actions project: sub-sea cable lifecycle study", 2015. [Online]. https://www.thecrownestate.co.uk/media/451414/ei-pfow-enabling-actions-project-subsea-cable-lifecycle-study.pdf

[38] Xue, Y., Thakhar, M., Theron, J. C., et al., "Review of the Breaker Failure Protection practices in Utilities". *In Protective Relay Engineers, 2012 65th Annual Conference for IEEE*, pp. 260-268, 2012.

[39] Q. M N Amjad, M. Zubair, G. Heo. "Modeling of common cause failures (CCFs) by using beta factor parametric model", *2014 International Conference on Energy Systems and Policies (ICESP)*, 2014.

[40] F S, B R, Pryor S, et al. "Analytical modelling of wind speed deficit in large offshore wind farms", *Wind energy*, vol.9, pp.39-53, 2006.

[41] L Huang, J Cao, K Zhang, et al., "Status and prospects on operation and maintenance of offshore wind turbines". *Proceedings of the CSEE*, vol.36, no.03, pp:729-738, 2016. (in Chinese)

[42] B Wang, X Wang, X Wang, et al., "Reliability Evaluation ofWind Plant Considering Collector Grid". *Proceedings of the CSEE*, vol.35, no.09, pp: 2105-2111, 2015. (in Chinese)

[43] A Sannino, H Breder, E K Nielsen. "Reliability of Collection Grids for Large Offshore Wind Parks". *9th International Conference on Probabilistic Methods Applied to Power Systems KTH*, Sweden, 2006.

[44] Noordzee Wind "Operations report 2009", [Online]., http://www.noordzeewind.nl/wp-content/uploads/2012/02/OWEZ_R_000_20101112_Operations_2009.pdf

[45] Liyu W., Yiqing X., "A preliminary study on typhoon damage to wind farm and the typhoon characteristics", *Wind Energy*, vol.5, pp.74-79, 2012. (in Chinese)

[46] X Jin, Y Hong, H Du. *Reliability analysis method of system with common cause failure*. Beijing, National defence industry press, 2008, pp.22-76. (in Chinese)